water

MDPI

Article

Groundwater Vulnerability Assessment in the Metaponto Coastal Plain (Basilicata, Italy)

Filomena Canora, Rosalba Muzzillo * and Francesco Sdao

Scuola di Ingegneria, Università degli Studi della Basilicata, 85100 Potenza, Italy; filomena.canora@unibas.it (F.C.); francesco.sdao@unibas.it (F.S.)

* Correspondence: rosalba.muzzillo@unibas.it

Abstract: This study aims at a groundwater vulnerability assessment of the Metaponto coastal plain, located in the Basilicata region (southern Italy). In the last century, intensive agriculture, zootechnical and industrial activities have significantly changed the plain. These changes led to negative impacts on the hydrogeological system intensifying the risk of the aquifer to pollution. The paper presents the assessment of the intrinsic vulnerability of the coastal aquifer carried out by the GIS-based application of the SINTACS method. It considers several aquifer parameters such as water table depth, effective infiltration, unsaturated conditions, soil media, aquifer media, hydraulic conductivity and topography. Furthermore, the anthropogenic influence in the study area was considered by applying the SINTACS-LU method, in which the parameter of land use (LU) was added. The SINTACS and SINTACS-LU vulnerability indexes were provided by summing the product of ratings and weights assigned to each parameter. The analysis of the intrinsic vulnerability map allowed for determining three classes ranging from low to high vulnerability. In both cases, the southeastern part of the coastal plain, closest to the sea, shows the highest vulnerability class, indicating that it is the most vulnerable to contamination due to the hydrogeological intrinsic factors. The wide central part of the study area shows a moderate class of vulnerability and the low class is scattered in small parts in the northern portion of the plain, which represents the areas less contaminable in space and time in the case of potential pollution. In the SINTACS-LU map, some areas classified as highly vulnerable in the SINTACS method show a minor vulnerability class. These areas are localized in natural and wooded sectors of the Metaponto plain, which are less populated, where human impact on the groundwater is minimal.

Keywords: groundwater vulnerability; SINTACS; land use; aquifer; Metaponto coastal plain

Citation: Canora, F.; Muzzillo, R.; Sdao, F. Groundwater Vulnerability Assessment in the Metaponto Coastal Plain (Basilicata, Italy). *Water* **2022**, *14*, 1851. https://doi.org/10.3390/w14121851

Academic Editor: Dimitrios E. Alexakis

Received: 5 May 2022
Accepted: 7 June 2022
Published: 9 June 2022

1. Introduction

In the 21st century, water scarcity and its pollution emerged as relevant problems worldwide. The protection of groundwater quantity and quality is therefore one of the main challenges to be undertaken in order to ensure people have availability of freshwater, which is highly threatened by overexploitation and contamination caused by anthropogenic activities and by the evident impacts of the climate-driven changes in water disposability. The authorities and stakeholders have an important role in the integrated planning of water resources, their management and protection, to ensure the best available drinking-water quality [1].

Nowadays, groundwater represents an important water supply resource subject to pollution, especially in agriculture-devoted areas having intensive activity involving the use of fertilizers and pesticides.

In the last decades, many studies of the international scientific community focused their attention on groundwater protection and management based on the groundwater vulnerability assessment. Groundwater vulnerability assessment has been widely recognized for its spatial prediction capability of groundwater to pollution [2–6]. It represents a

relevant tool for the protection of groundwater resources and results in being useful for their planning and management.

The intrinsic vulnerability map provides valuable information to stakeholders interested in preventing groundwater degradation, especially in the presence of current climate and environmental changes [7].

Different definitions of groundwater vulnerability were proposed [8–10]. The intrinsic vulnerability of groundwater to contamination can be defined as the sensitivity of the aquifer systems, in their different geometric and hydrodynamic settings, to ingest and spread a pollutant, even mitigating its effects, and with the ability to impact the groundwater quality [11].

Based on this definition, the aquifer vulnerability is assessed independently of the nature of pollutants resulting from human activities but referring to the geological and hydrogeological aquifer characteristics [12].

Currently, several approaches have been proposed for assessing the vulnerability of groundwater.

Different authors [5,13–15] and references therein proposed comprehensive reviews about advanced approaches for the groundwater vulnerability assessment, highlighting the status and challenges of groundwater protection.

In recent years, the different approaches have been greatly enhanced since the advent and the improvement of Geographic Information Systems (GIS), which made the storing, elaboration, interpretation, and representation of a wide amount of georeferenced data to assess groundwater vulnerability over the large spatial scales simpler than in the past [16].

Process-based models (e.g., SUTRA [17], PRZM [18], LEACHP [19], GLEAMS [20], MT3DMS [21] and Hydrus [22]), overlay and index methods (e.g., DRASTIC [23], SINTACS [24–26], EPIK [27] and COP [28]), statistical techniques [29,30] and hybrid procedures [31] are the relevant approaches elaborated in the literature to evaluate aquifer vulnerability [10,14].

All these method and technique typologies show different benefits and drawbacks. Although process-based models can create a transient representation of groundwater quality [32–35], they are typically utilized on small-scale domains due to the need for high quality and frequency data, as well as the high computing time and demand.

Advanced statistical techniques, successfully integrated with GIS, have been applied in recent times by several researchers [36,37]. The disadvantages of these methods can be found in the requirement for large and high-quality datasets.

Overlay and index methods can be easily implemented, modified and updated, can be applied to wide domains, and usually do not need large amounts of data [5,38]. However, they could be affected by subjectivity in rating assignment.

Hybrid procedures, which primarily combine overlay and index methods with statistical analysis, aim to overcome their limitations [39,40].

Many overlay and index procedures and methods have been set based on parameters derived from hydrogeological data represented by ratings and weights [41,42].

The purpose of this study was the assessment of groundwater vulnerability to pollution of the coastal plain of Metaponto (Figure 1) using the GIS-based SINTACS method [3,43,44] and a modified SINTACS method that was obtained by adding the parameter of land use (LU) [45–47]. The applications are carried out by assigning ratings and relative weights to each hydrogeological parameter. The main aim of this study is to improve the knowledge in the groundwater vulnerability assessment of the Metaponto coastal plain aquifer system characterized by intensive agricultural vocation.

The applications allow to better focus on groundwater-related programs and strategies to promptly assess potential groundwater quality impacts caused by anthropogenic sources, i.e., the intensive agricultural practices, and, therefore, provide the optimization of land use.

2. Study Area

The Metaponto coastal plain, located in the southern part of the Basilicata region (Italy), extends for about 40 km along the Ionian coast and covers an area of about 280 km^2.

The study area morphology is characterized by smooth marine terraces engraved by river valleys, which constitute the surface drainage network and by plains close to the sea. The study area is characterized by an average elevation of about 20 m a.s.l. The climatic conditions are typical of a Mediterranean climate characterized by dry summers and mild, wet winters. Precipitation is scarce and concentrated mostly in the winter season, the mean annual value is about 520 mm. In summer, the temperature reaches values higher than 32 °C and a minimum of about 18 °C. The winter temperatures range from 3 °C to 12 °C. The mean annual value of temperature is equal to 16.3 °C.

The morphology of the study area highlights, from the coastline moving inland, different zones. According to a general coastal model [48], the coastal subaerial sector can be divided into foreshore primarily constituted by a limited sandy deposit stretch, and backshore affected by dunes, striking mainly parallel to the shoreline, and flat variable-width zones, ranging from 2 to 5 km, constituted by fluvial deposits. The inland areas present a staircase of marine terraces succession, almost parallel to the coastline, crosscut by different rivers (Bradano, Basento, Cavone, Agri and Sinni) with an NW-SE trend.

Due to the particular morphology of the territory, the rivers caused flooding and marsh areas in the peri-coastal environment. Starting from 1950, the hydraulic arrangement and land reclamation of the Metaponto coastal area, carried out by the Irrigation and Land Development Authority, have contributed to the development of the entire plain. Nowadays, the plain represents an important area for the economic growth of the region, especially regarding intensive agriculture production and tourism. During the 20th century, reclamation works and the development of modern irrigation systems favored agricultural and industrial activities, which, together with groundwater exploitation and climate change impact, have strongly modified the hydrogeological conditions of the plain.

3. Geological and Hydrogeological Setting of the Study Area

The Metaponto coastal plain, from a geological viewpoint, is located along the Ionian coastal area of the Basilicata region, in the southernmost part of the Bradanic Foredeep that lies between the eastern front of the Apennine chain and the western sector of the Apulia foreland. From the Middle–Upper Pleistocene, the interaction of regional uplift and eustatic sea-level fluctuations favored the evolution of marine terraces [49–53] (Figure 1).

The marine-terrace deposits (Middle–Upper Pleistocene), constituted by thin gravel, sand and silt wedges organized in superimposed layers, unconformably overlie the substratum made by marine grey-blue silty clays of the sub-Apennine Clays Formation (Upper Pliocene?–Middle Pleistocene), outcropping mainly along the deeper incision of the fluvial network [51,53].

The flat surfaces of the marine terraces, having a similar trend to the current coastline and representing the ancient coastlines of the different sea level standing phases, are crosscut by the fluvial incisions of the Sinni, Agri, Cavone, Basento and Bradano rivers (from SW to NE) [56] (Figure 1).

The Alluvial, transitional and marine deposits (Upper Pleistocene?–Holocene), extensively present in the coastal plain, overlay the marine grey-blue silty clays that crop out in limited portions along the sides of the rivers [51]. Silty-clayey and sandy silts layers, with interspersed sandy layers, characterize the alluvial deposits, present mainly along the river valleys and on flood plains. The transitional and marine deposits are characterized by gravel, sand and silt layers of the deltaic and beach depositional environment, unevenly distributed mostly in the coastal plains and prograded up to the present Coastal Deposits [51] (Figure 1).

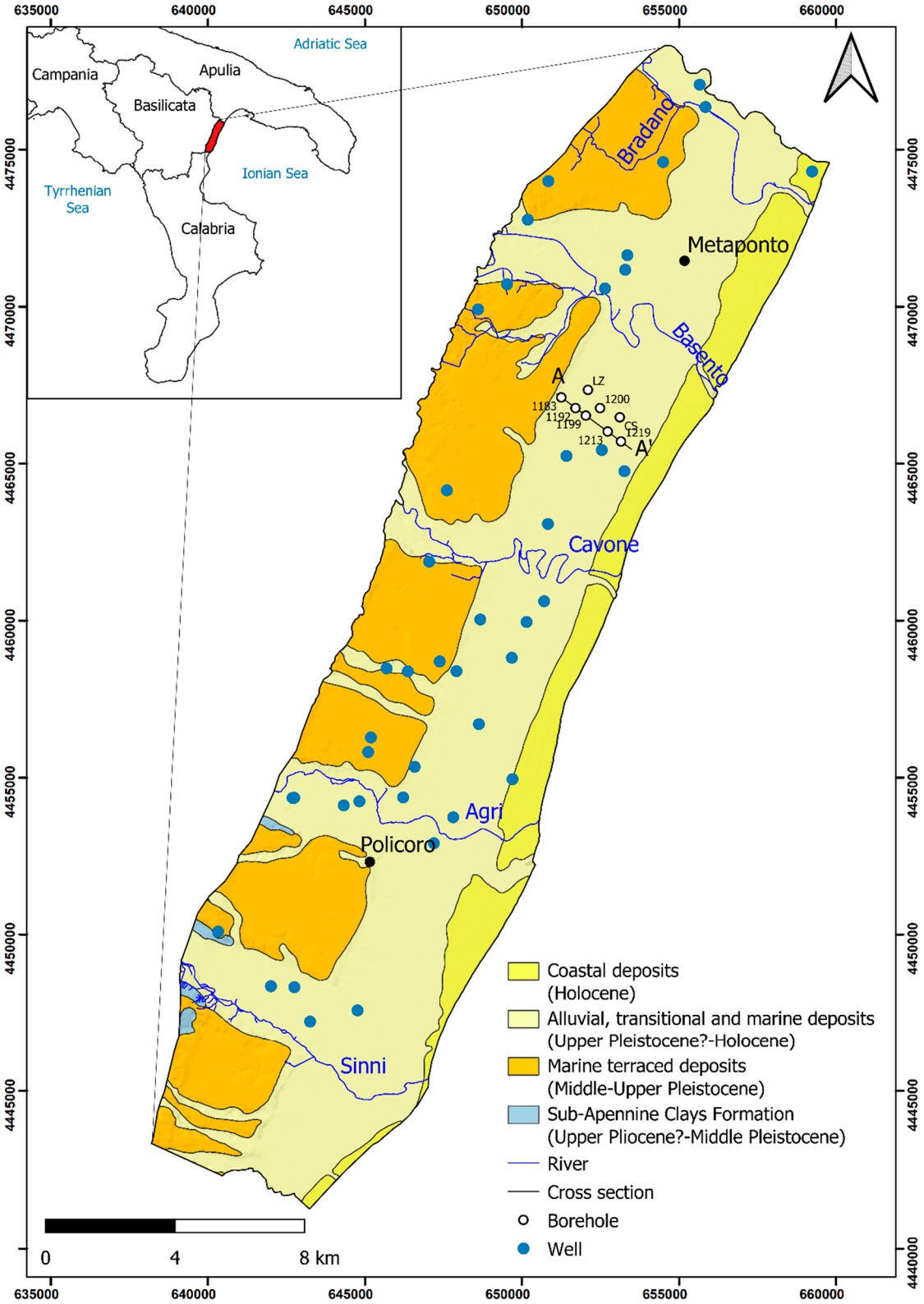

Figure 1. Schematic geological map of the Metaponto coastal plain (adapted from Geological Map of Italy 1:100,000 scale [54] and 1:50,000 scale [55]).

The Coastal Deposits defined the sandy beaches, which become sandy or gravely sandy, with pebbly lenses towards the Sinni River [57]. Coastal dunes and marshy areas made up of weakly cemented sands border the beaches inland. Wetlands and coastal dunes

made up of compact and weakly cemented sands delimit the beaches in the hinterland (Figure 1).

The lithostratigraphic setting of the Metaponto Coastal Plain, derived from the cross-section AA′ (Figure 2) of the Geological Map of Italy 1:50,000 scale [55] and realized based on several datasets referring to the boreholes present in the study area, highlight different stratigraphic units [55] (Figures 1 and 2). From the bottom to the top, t is composed of the irregular depth of shelf-transition clayey, clayey-silty, and clayey-sandy deposits, locally with intercalations of discontinuous gravel levels, belonging to sub-Apennine Clay Formation (Middle–Pleistocene), reaching about 120 m b.s.l. in correspondence with the paleo river valleys [53], mainly filled by estuarine deposits [49,51]. Fluvial and/or deltaic sandy-gravelly deposits with locally clayey and clayey-silty deposits belonging to marine-terrace deposits (Upper Pleistocene) characterize the second unit.

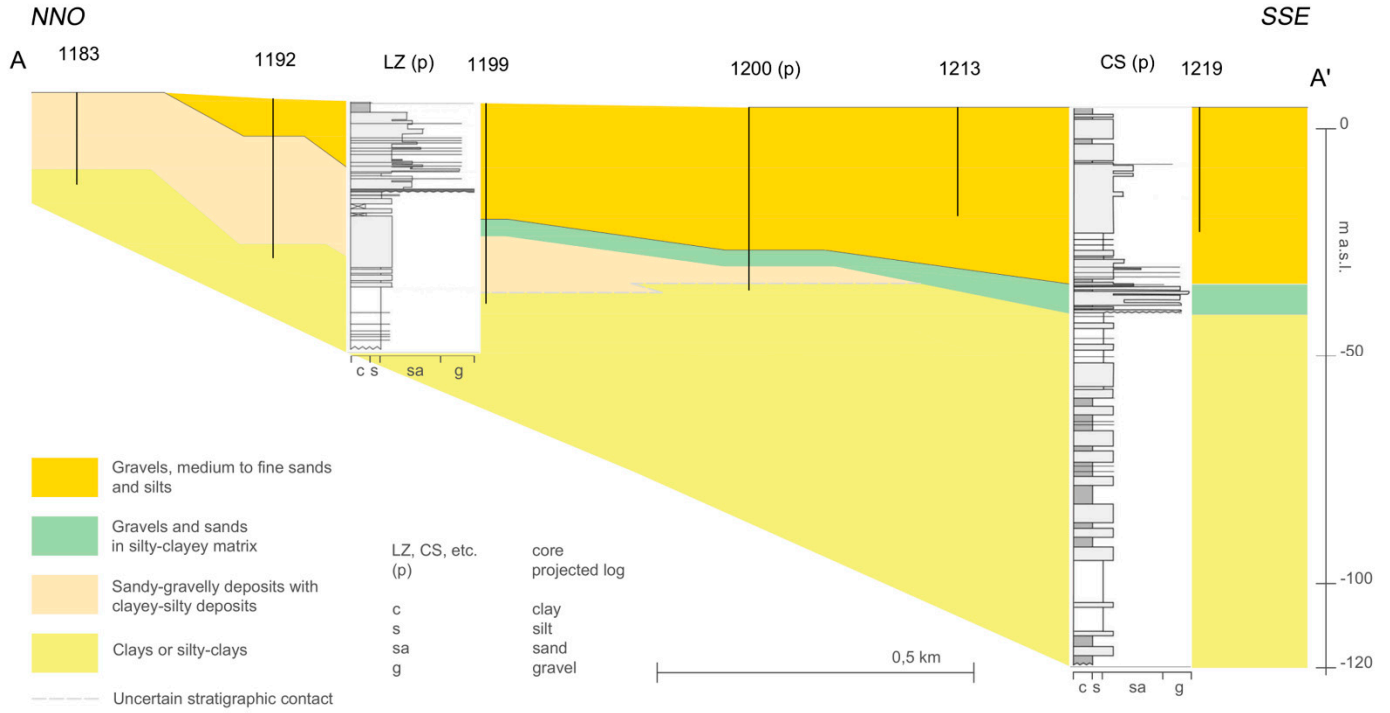

Figure 2. Schematic cross section AA′ (see Figure 1 for location) of the Metaponto coastal plain stratigraphic units (adapted from Geological Map of Italy 1:50,000 scale [55]).

The last two lithostratigraphic units constitute the buried and outcropping coastal prisms of Metaponto, both belonging to the Alluvial, transitional, and marine deposits. Sandy, gravelly and silty deposits constitute the buried prism (Upper Pleistocene). They have filled the paleo river valleys during low-stand of sea level, the depth of which ranges between 30 and 40 m below the current sea level. These deposits, laterally discontinuous, lie by erosional surface on the substrate and the sandy-gravelly deposits. The outcropping deposits of the coastal prisms (Upper Pleistocene-Holocene) constitute the upper unit. These medium-to-fine sandy, gravelly and silty deposits of a continental to transitional environment during a lowstand of relative sea-level, filled the incised paleovalleys, and, subsequently, the aggradation took place to form the current Metaponto coastal area.

The peculiar hydrogeological structure of the coastal plain of Metaponto reflects the complex and articulated geological and stratigraphic context. The distinctive boundary conditions of the groundwater flow have been determined by the spatial distribution of the different formations and the geomorphological evolution of the entire area. The grey-blue clays, characterized by very low hydraulic conductivity, constitute the bottom of the entire aquifer system [58,59]. Different mostly unconfined aquifers can be distinguished [60,61]: two aquifer typologies are located in the marine terraced deposits and alluvial deposits of

river valleys. The third one is located in the interfluvial coastal plain: the plain deposits create a shallow sandy aquifer, which is widely exploited. The hydraulic conductivity of the marine terraced deposits is generally medium, with maximum values of 10^{-3} m/s [59], in correspondence with the sandy and gravelly sediments, and becomes very low for silty-clayey levels. In the coastal plain, alluvial sediments are more distinctly sandy and form transitional deposits consisting of sand, gravel and silt in layers variously distributed in space. On a large scale, the mean and median values of the hydraulic conductivity of the plain deposits are 2.28×10^{-4} and 6.53×10^{-5} m/s, respectively [59,60]. The hydraulic conductivity can locally decrease to very low values for the silty-clayey levels.

Even if the direct rainfall infiltration in the study area is scarce, both due to the low rate of effective rainfall and the effect of the low-permeability soils [59,60], the groundwater of the coastal aquifer is assured by the discharge from upward aquifers, in which the recharge areas are localized, and by the river leakage. The trend of the piezometric surface, almost striking parallel to the coastline, highlights that the preferential groundwater flow pathways are direct from the marine terraces and the rivers' valley alluvial deposits to the Ionian coast.

4. Materials and Methods

4.1. SINTACS and SINTACS-LU Methods

The SINTACS method, belonging to the GIS-based overlay and index approaches [3], was selected and applied in the Metaponto coastal plain to assess the intrinsic vulnerability to pollution. The SINTACS method, widely applied for determining groundwater vulnerability, represents the evolution of the DRASTIC method [23] suitable to the hydrogeological Mediterranean environments [45,62].

In this method, the hydrogeological scenarios characterized by the weights attributable to each parameter are more numerous and flexible than in the DRASTIC, which provides strings of weights for only two hydrogeological contexts. The index-based SINTACS method is easy to apply, low-cost, requires limited datasets and low computational time, and provides adequate reliability and accuracy of the results [42].

The acronym "SINTACS" derives from the initials of the Italian words that express the input conditioning factors used by the method to assess the intrinsic vulnerability of the Metaponto coastal plain. These parameters are: (i) S (Soggiacenza) water table depth; (ii) I (Infiltrazione efficace) effective infiltration; (iii) N (Non-saturo) unsaturated zone; (iv) T (Tipologia della copertura) soil media; (v) A (Acquifero) aquifer characteristics; (vi) C (Conducibilità idraulica) hydraulic conductivity and (vii) S (Superficie topografica) topographic slope.

Based on the structure of the SINTACS method [3,26,44], each hydrogeological parameter is divided into different classes, to which it is assigned ratings and relative weights.

The SINTACS index is provided using the following Equation (1):

$$SINTACS\ index = S_rS_w + I_rI_w + N_rN_w + T_rT_w + A_rA_w + C_rC_w + S_rS_w. \quad (1)$$

In this study, one more parameter was considered in the SINTACS method with the aim to improve the accuracy in representing groundwater vulnerability: the land use (LU) was included to take into account the anthropogenic influence in the study area. Land cover plays a key role in relation to the pressure exerted on groundwater quality by industrial, urban and vegetation land uses, posing a serious threat to groundwater resources [19,20]. This parameter was ranked depending on land use and weighted with a 5 value (Table 1). The modified SINTACS index was computed using the following Equation (2):

$$SINTACS - LU\ index = S_rS_w + I_rI_w + N_rN_w + T_rT_w + A_rA_w + C_rC_w + S_rS_w + LU_rLU_w \quad (2)$$

where for both equations, S, I, N, T, A, C, S and LU are the above-reported parameters; r is the rating value; w is the weight assigned to each parameter.

Table 1. Ranges, ratings and weights of SINTACS and SINTACS-LU parameters (modified from [24,25,44]).

SINTACS Parameters	Range	Rating	Weight
S—water table depth (m)	5.0–10	6	5
	3.0–5.0	7	
	1.5–2.0	9	
	1.5	10	
I—effective infiltration (mm/year)	0–50	1	5
	50–65	2	
	>65	3	
N—unsaturated zone	Clay deposits	2	4
	Fine alluvial deposits	4	
	Medium-fine alluvial deposits	5	
	Coarse alluvial deposits	6	
	Sandy coastal deposits	7	
T—soil media	Clay loam	3	5
	Silty-clay loam	4	
	Loam	5	
	Sandy loam	6	
	Sandy	8	
	Coarse sand	9	
A—aquifer media	Clay	3	2
	Medium-fine alluvial complex	6	
	Coarse alluvial complex	7	
	Sandy complex	8	
C—hydraulic conductivity (m/s)	$6.53 \cdot 10^{-5}$	5	2
	$2.28 \cdot 10^{-4}$	7	
	$5.69 \cdot 10^{-3}$	9	
S—topographic slope (%)	>25	1	3
	20–25	2	
	17–20	3	
	14–17	4	
	11–14	5	
	8–11	6	
	6–8	7	
	4–6	8	
	2–4	9	
	<2	10	
LU—land use	Pastures, Forests	3	5
	Beaches, Dunes, Sands	4	
	Olive groves, Vineyards	5	
	Mining areas	6	
	Annual crops, Fruit trees, Urban areas	7	
	Industrial areas, Wetlands	8	
	Intensive agriculture	9	

The data implementation and processing were successfully performed in a GIS environment to assess the vulnerability of groundwater with the SINTACS methodologies. The advantages of GIS are identifiable in the ability to store, organize and analyze uniquely georeferenced spatial geographic data and the efficiency in combining different layers of information. Eight layers (one for each parameter) were prepared and processed to produce the groundwater vulnerability maps and then reclassify the indexes (Figure 3).

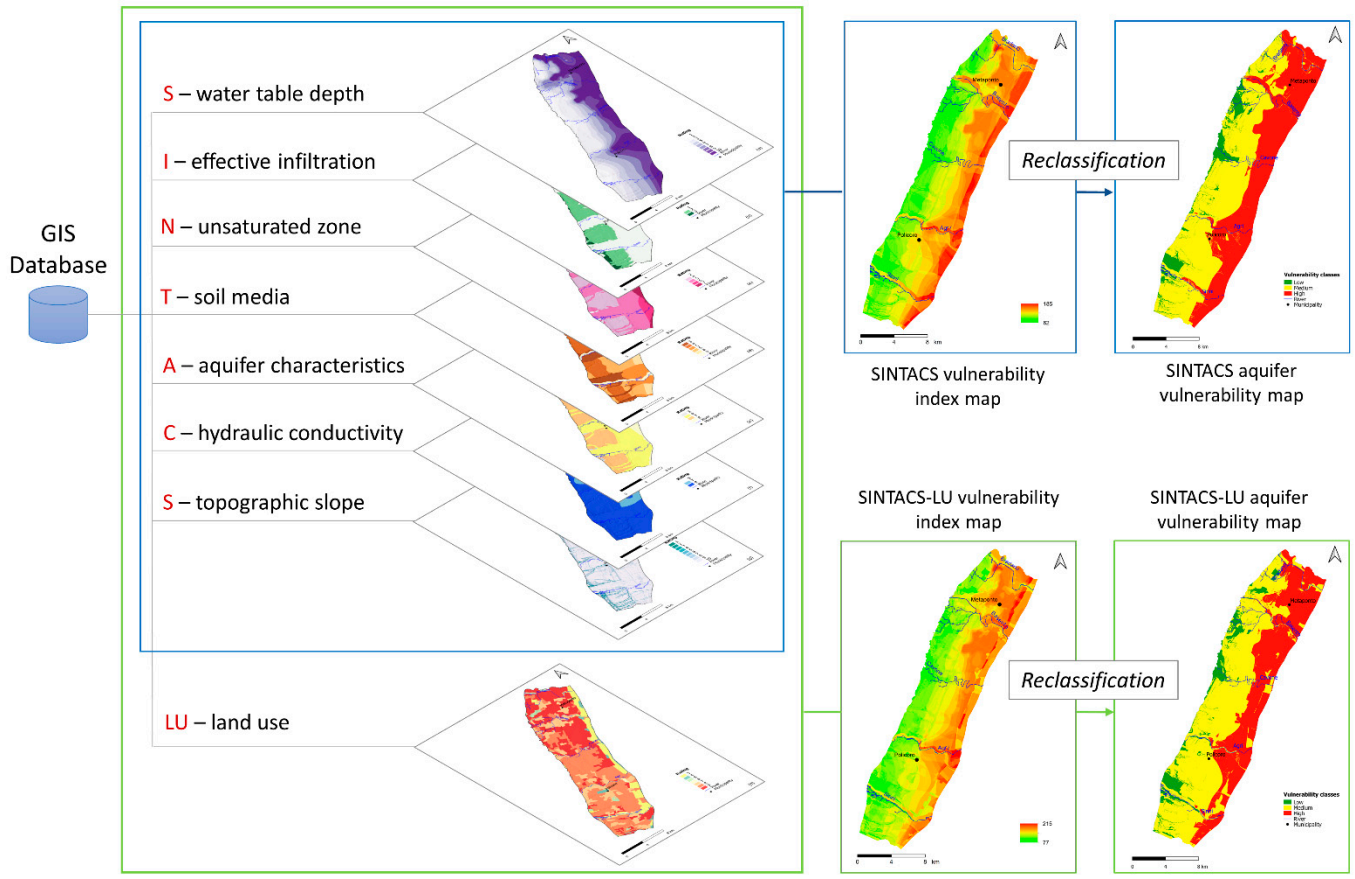

Figure 3. Methodology flow chart for SINTACS and SINTACS-LU methods.

Each parameter is evaluated depending upon its relative importance to the potential intrinsic vulnerability and indexed by attributing rating ranges from 1 to 10, according to Table 1.

To each parameter is subsequently attributed a multiplying weight ranging from 1 to 5 (Table 1). The SINTACS method proposes six different strings of weights related to the different hydrogeological and anthropogenic conditions, to which the Land Use (LU) parameter was added (Table 2). The choice of the string of weights "Nitrates" was made considering the mainly agricultural vocation of the study area [44]. To the relevant parameters is assigned a weight of 5, whereas the less important are assigned a weight of 2 (Table 1). Finally, the vulnerability indexes are calculated by Equations (1) and (2). The higher intrinsic vulnerability to pollution is indicated by the higher SINTACS index.

Table 2. Strings of multiplier weights given for SINTACS (modified from [44]).

Parameter	Normal	Severe	Seepage	Karst	Fissured	Nitrates
S	5	5	4	2	3	5
I	4	5	4	5	3	5
N	5	4	4	1	3	4
T	3	5	2	3	4	5
A	3	3	5	5	4	2
C	3	2	5	5	5	2
S	3	2	2	5	4	3
LU	5	5	5	5	5	5

The data collection and the surveys were carried out in the overall Metaponto plain. The elaboration and preparation of the SINTACS thematic layers were performed with QGIS software and rasterized with grids of 5 m cell size, using the Kriging approach [63]

(Figure 3). The Kriging technique provides an efficient method for the interpolation of the limited number of observations such as wells, rainfall and temperature data for hydrogeological water balance, hydraulic conductivity determined in punctual sites and for preserving the theoretical spatial correlation [64]. The elaborated data were retrieved as follows.

4.1.1 The water table depth (S) is the distance between the ground surface and the water table and indicates the depth that a contaminant must pass through to reach groundwater [46]. It affects the contaminant in biological and chemical reactions, and the time required to reach groundwater [47]. A low depth to groundwater leads to a higher vulnerability rating. This parameter originated from 42 selected monitored wells' water level measurements located in the study area (Figure 1). The layer was elaborated based on their localization and the water table depth spatial distribution map was obtained through the Kriging interpolation technique in terms of raster data.

4.1.2 The effective infiltration (I) parameter, is the amount of infiltration that penetrates from the ground surface and reaches the aquifer, and can transport contaminants to the water table through the unsaturated zone. If the effective infiltration increases, the contamination potential of groundwater will rise too. The effective infiltration in the study area was evaluated by the estimation of the hydrogeological budget components applying the inverse hydrogeological water balance approach [65,66]. The effective infiltration results directly related to groundwater contamination. The hydrogeological water balance of the study area, due to the low hydraulic conductivity of the outcropping soils [67] and the unfavorable climatic conditions, shows low values of the effective infiltration rate.

4.1.3 Unsaturated zone (N) characteristics and thicknesses influence groundwater intrinsic vulnerability. The vadose zone included between the bottom of the soil horizon and the water table controls the dilution and the contaminant rate that reach the saturated zone. The ratings assigned to the unsaturated zone classes are given in Table 1. This parameter was elaborated considering lithological characteristics of the geological formations and available stratigraphic data of wells.

4.1.4 Soil media (T) affects the transport mechanisms of the contaminant from the soil surface to the water table. Aquifer potential vulnerability depends upon soil characteristics such as soil organic materials percentage, texture, and permeability [46]. Soil media plays a key role in assessing the vulnerability index of groundwater as it restricts the vertical flow of contamination into the subsurface. In addition, it has a significant impact on the amount of recharge that flows through the soil. Soil data was taken from the pedological map of the Basilicata Region [68].

4.1.5 The aquifer media (A) parameter refers to the characteristics of the saturated zone, such as the porosity rate, particle types and size [46]. The relative layer was prepared using geological data, lithological maps and stratigraphic borehole data available for the study area. The ratings assigned to the aquifer media parameter are reported in Table 1.

4.1.6 Hydraulic conductivity (C) measures the capability of the aquifer to transmit water and controls the rate at which the groundwater will move when subjected to a given hydraulic gradient. This parameter controls the transport and distribution of contaminants from the injection point inside the saturated zone [46]. High permeability allows more infiltration rates and higher concentrations of contaminants to reach the saturated zone. The high permeability of the aquifer system provides a high vulnerability index. The hydraulic conductivity values were obtained from many pumping tests carried out in the study area in the last twenty years [59]. These values were used to elaborate the hydraulic conductivity map.

4.1.7 Topography (S) indicates the slope of the topographic surface and influences the vulnerability assessment in relation to the fact that water and pollutant can run off or stay on the surface for a time long enough to infiltrate. For low topographic slope, the infiltration rate is higher, and, consequently, contaminants have a greater probability of infiltrating the aquifer. With larger slopes, the infiltration capacity decreases and the surface is less vulnerable to groundwater contamination. Thus, by decreasing the slope, the

vulnerability of the aquifer increases. The slope map was derived from the digital elevation model data covering the investigated area and downloaded from the Basilicata Region website with a spatial resolution of 5 m and it is expressed as a percentage of the steepness.

4.1.8 Land use (LU) impact on vulnerability was considered by including the land use parameter in the SINTACS approach. The land use data were derived from Corine Land Cover 2018 [69]. In the study area, the groundwater quality is subjected to degradation due to the anthropic impact of the urban, agricultural and industrial pressures. In particular, the Metaponto coastal plain aquifer system is conditioned by intensive agricultural activities and other pollution sources.

4.2. Sensitivity Analysis

The selection of ratings applied to the parameters included in SINTACS and SINTACS-LU methods is inevitably linked to subjectivity. Because such a choice significantly impacts on the final vulnerability maps, the sensitivity analysis can be performed to understand the influence of the input parameters on the output, assess the consistency of the results, individuate which variables are more relevant and hence require more thorough information and accuracy [70].

In this research, map removal and single variable analysis were the two types of sensitivity analysis performed with a quick and low-cost GIS-based approach.

4.2.1. Map Removal

The goal of the map removal analysis is to figure out if all the parameters are necessary for the computation of the vulnerability index, or if one or more of the parameters may be deleted without having a significant impact on the outcome. The analysis was performed for both SINTACS and SINTACS-LU methods by deleting one parameter at a time and assessing the effect on the output by calculating the following sensitivity measurement in each cell in which the study area was discretized [71–73]:

$$S = \left(\frac{\left| \frac{V}{N} - \frac{V'}{n} \right|}{V} \right) \cdot 100 \quad (3)$$

where S is the sensitivity measurement expressed in terms of a variation index, V is the unperturbed vulnerability index obtained using all the parameters, V' is the perturbed vulnerability index computed using a lower number of input layers, N and n are the number of parameters considered to calculate V and V', respectively. The average variation index of all cells for each parameter can be used to identify which parameter could have less influence on the outcome if omitted [72]. Any parameter with a lower overall average index value has less influence. A cell with a high or low index for a removed parameter will show a greater or smaller influence on the outcome, accordingly.

4.2.2. Single-Parameter Sensitivity Analysis

The single-parameter sensitivity analysis is a cell-based process, too [70]. The theoretical weight assigned by the SINTACS and SINTACS-LU methods to each parameter was compared to the "effective" or "actual" weight, which was calculated as follow:

$$W = \frac{P_r P_w}{V} \cdot 100 \quad (4)$$

where P_r and P_w are the rating and weight of the P parameter, respectively, and V is the vulnerability index as computed in Equations (1) or (2).

The goal of this analysis was to determine which parameter had the highest effective weight and therefore provided higher values of the vulnerability indexes when its spatial variation throughout the entire study area was considered [70,73].

5. Results and Discussion

5.1. Conditioning Indicators

5.1.1 The depth of the water table (S) appears to be one of the parameters that most significantly impacts groundwater vulnerability. Shallow aquifers are commonly more vulnerable than deep aquifers, where infiltrating contaminants require a longer interaction time with unsaturated media, and biogeochemical reactions can reduce their impact. The data on the groundwater level were acquired from 42 wells utilized for agricultural and domestic supply, and monitoring aims (Figure 1). These data were elaborated to determine water table depth (S). The observed data highlight that the water table is relatively shallow and the water depth ranges from 1.5 to 8 m. Kriging method was used for the interpolation of the punctual data. The depth of the water rasterized layer was ranked by assigning four classes of ratings, listed in Table 1, and its spatial distribution is shown in Figure 4a. It is evident that the shallow aquifer will result in a higher potential intrinsic vulnerability, whereas the deep aquifer is relatively less impacted by contamination. In the investigated area, the southeastern sector shows high intrinsic vulnerability due to the higher rating of this parameter (Figure 4a).

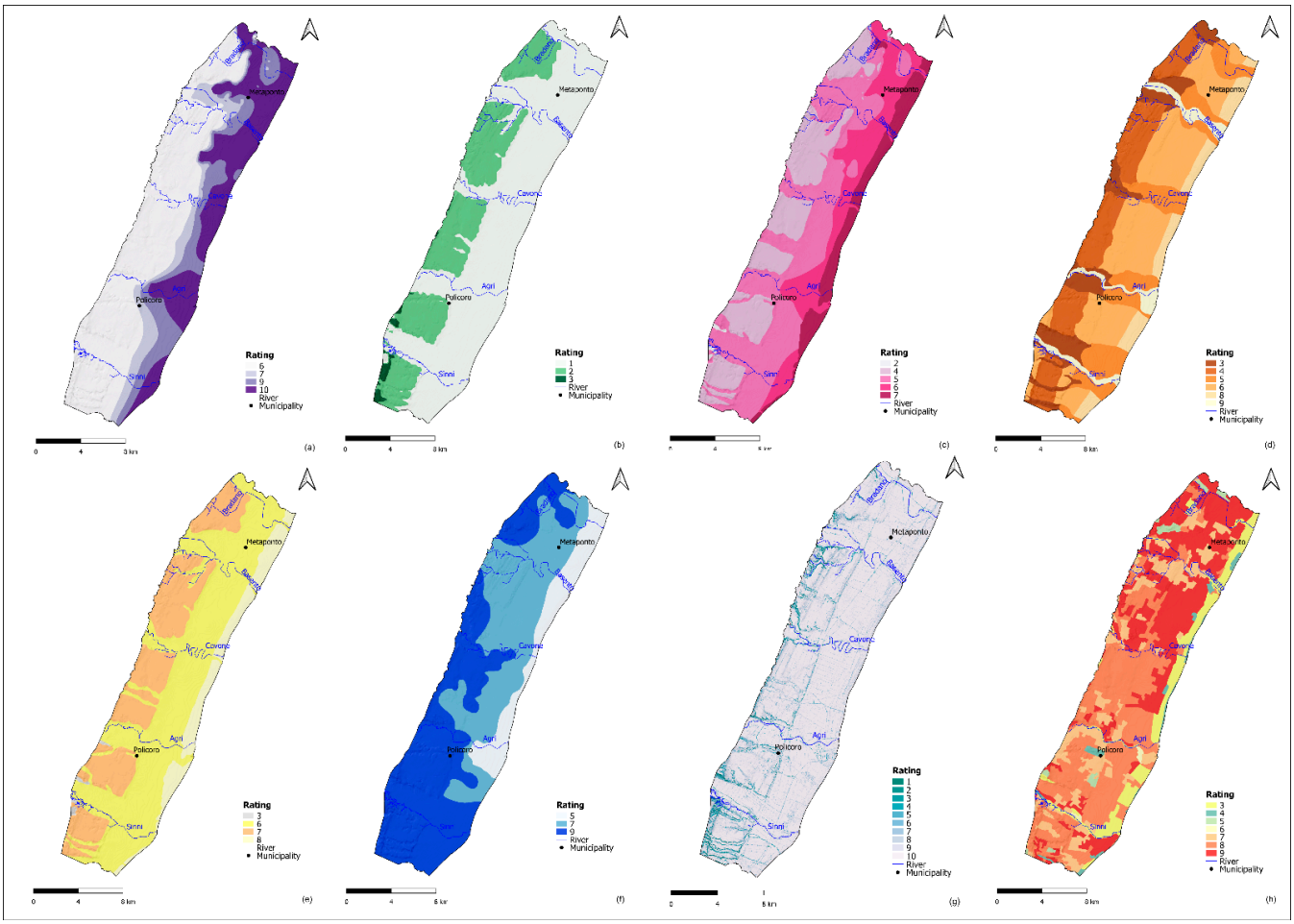

Figure 4. The thematic maps for SINTACS and SINTACS-LU methods: (**a**) water table depth; (**b**) effective infiltration; (**c**) unsaturated zone; (**d**) soil media; (**e**) aquifer media; (**f**) hydraulic conductivity; (**g**) topography; (**h**) land use.

5.1.2 Effective infiltration (I) is the amount of water that infiltrates through the unsaturated zone and reaches the aquifer. The infiltration was estimated using the inverse hydrogeological water balance [24,74]. This methodology consists of the infiltration estimation starting from the analysis of climate data, such as rainfall and temperature, topographic

and hydrogeological parameters, such as the altimetry and the hydrogeological complexes characteristics of the study area. The GIS-based method allows to obtain the spatial distribution of the effective infiltration rate in the hydrogeological basin [65,66]. In QGIS software, daily rainfall and air temperatures series were collected and elaborated for the period 2000–2015. In the hydrogeological basin, the mean annual rainfall is about 538 mm. The results of the GIS-based distributed inverse hydrogeological water balance procedure show that the actual evapotranspiration (equal to 465 mm) provides an effective infiltration rate equal to 52 mm/year, which is equivalent to about 1080 L/s. The mean annual value of direct runoff is equal to 21 mm/year [67] (Figure 4b).

5.1.3 The unsaturated zone (N) or vadose zone represents the thickness defined by the soil horizons and the groundwater table. The attenuation capacity of the contaminants is strongly affected by the unsaturated media properties that influence many processes such as biodegradation, diffusion and chemical reactions. The possibility of groundwater contamination can increase with small thicknesses of the vadose zone and high permeability, consequently enhancing the intrinsic vulnerability of the aquifer. The values of the parameter N were obtained from well stratigraphic profiles integrated with geological maps and geophysical surveys [60]. The N parameter ratings range from 2 to 7 (Table 1). The results highlighted that among the vadose zone classes: Medium-fine alluvial deposits (rating 5), Fine alluvial deposits (rating 4), Coarse alluvial deposits (rating 6), Sand coastal deposits (rating 7) and Clay deposits (rating 2) cover around 42%, 26%, 20%, 11% and 1% of the total study area, respectively (Figure 4c).

5.1.4 Soil media (T) is the uppermost vadose layer where biological activities are significant. Soil characteristics condition the behavior and the amount of the contaminants that can reach the water table [75]. The presence of organic components, the thickness of soil media, and the grain size can significantly impact the contaminant's attenuation mechanisms. Different textures of soil media (coarse sand, sand, sandy loam, loam, silty clay loam and clay loam) are present throughout the study area (Figure 4d).

5.1.5 Aquifer media (A) describe the components' characteristics of the saturated zone such as the porosity rate, particle types and grain size, and the processes that take place below the piezometric level. Basically, these processes are hydrodynamic dispersion, dilution, absorption and chemical reactions between the aquifer media and the contaminants [61]. The aquifers of the study area are mainly unconfined. The results showed that the medium–fine alluvial complex covers 59% of the study area. Alluvial, sandy and fine sand complexes cover the 29.5%, 11%, and 0.5%, respectively (Figure 4e). The analysis of the thematic layer suggests that the south-eastern portion of the study area (closest to the coast) is under high intrinsic vulnerability.

5.1.6 Hydraulic conductivity (C) is defined as the ability of the fluid to pass through the aquifer media. This physical property expresses the groundwater flow and mobile contaminants rate that can reach the water table [23]. High hydraulic conductivity gives higher potential groundwater contamination and, therefore, greater intrinsic vulnerability. The hydraulic conductivity of the study area ranges from 10^{-5} to 10^{-3} m/s (Table 1, Figure 4f).

5.1.7 Topography (S) is expressed by the variability of a land surface slope as a percentage. This study used DEM data for extracting the slope information. Low-slope areas can be more vulnerable to pollution as they retain water longer and contaminants are more likely to infiltrate. More than 70% of the study area has a slope class of 0–2%, corresponding to flat areas, which are given the highest rating and, therefore, have a significant impact on intrinsic vulnerability (Figure 4g).

5.1.8 Land use (LU) of the study area is constituted as urban, industrial and vegetation land cover [69]. The quality of groundwater resources in the Metaponto coastal plain is mainly threatened due to population growth, intensive agricultural, industrial and urban activities. The development of agricultural activities has resulted in a general increase in the size of cultivated areas. The vegetation covers areas largely characterized by agricultural crops. The plain is characterized by the presence of forests and pasture located mainly in

the southeastern part. Along the coast, the Mediterranean maquis takes on the prevailing vegetational characteristics. The Mediterranean maquis is replaced by the garrigue, a low, soft-leaved scrubland, in the areas with unfavorable climatic and soil conditions and where anthropogenic pressures, such as fire and grazing, are stronger [69,76]. Some areas are characterized by parcels allocated to permanent crops, mainly vineyards, olive trees and sown land. Permanent crops are present on all plain; the coastal area is mainly covered by orchards. Inadequate or intensive farming practices have aggravated the degradation phenomena currently underway, mainly in the study area characterized by unfavorable climatic conditions [69,76]. The land use impact on the vulnerability was taken into account by adding the LU parameter to the SINTACS method (Table 1).

5.2. SINTACS Vulnerability Index

The SINTACS and SINTACS-LU indexes were determined using Equations (1) and (2), and the resulting intrinsic vulnerability indexes are represented in Figure 5a,b.

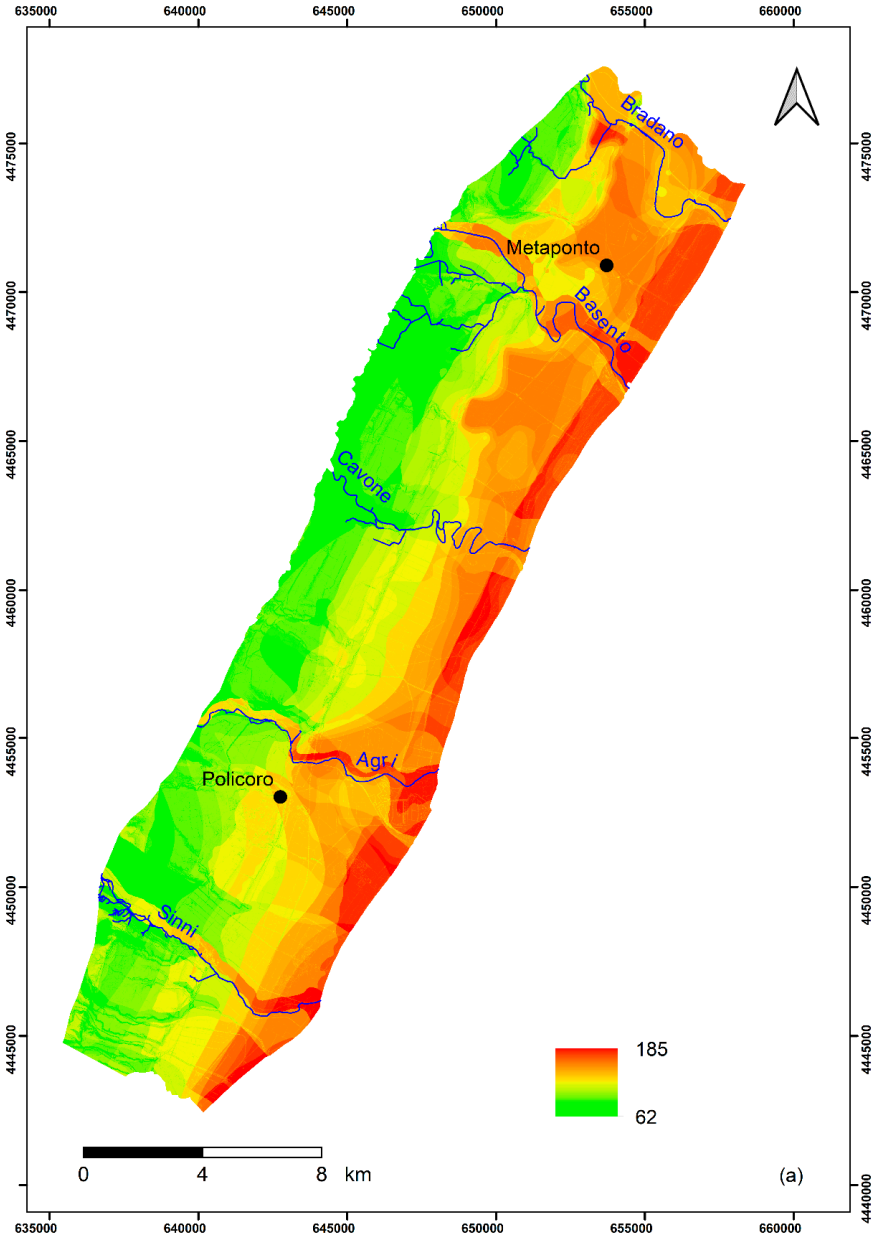

Figure 5. *Cont.*

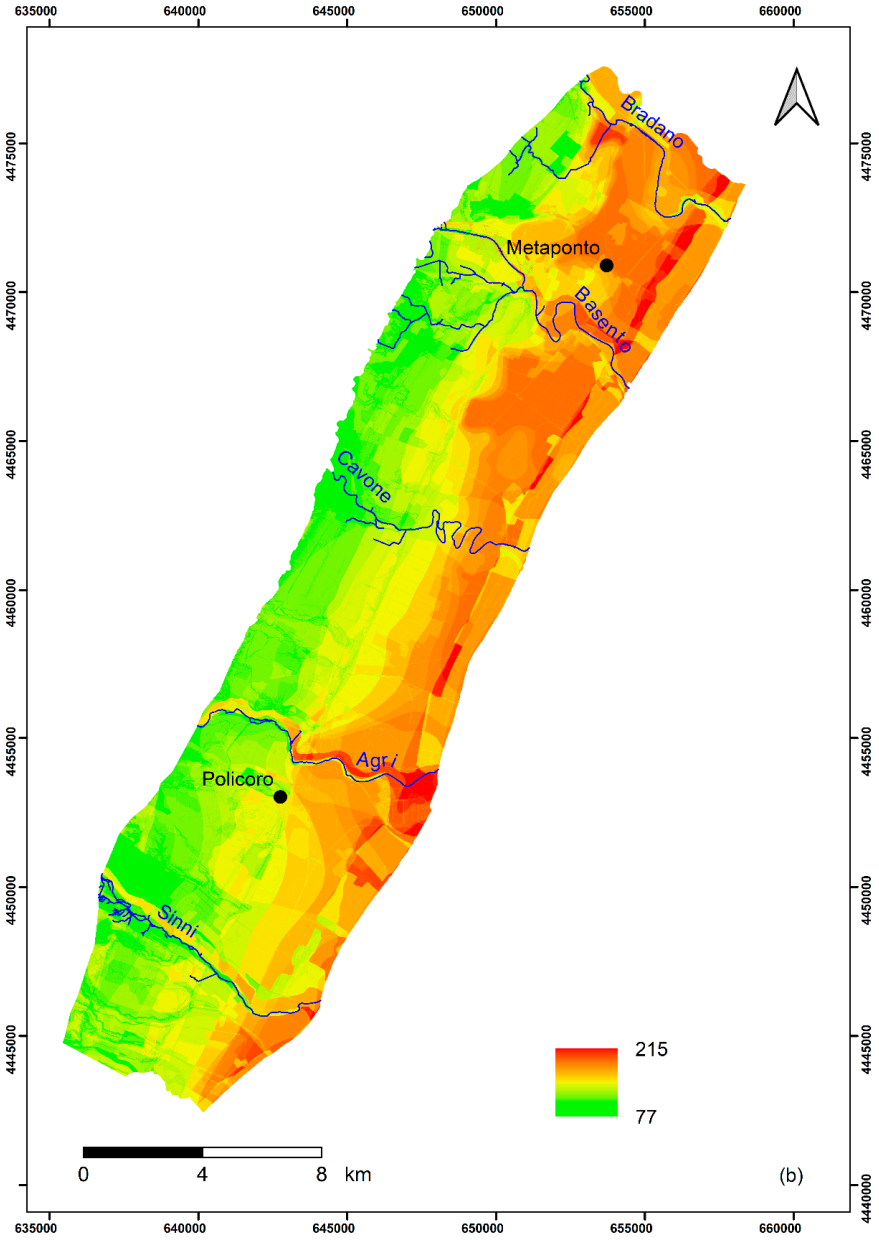

Figure 5. Groundwater vulnerability indexes elaborated with: (**a**) SINTACS method and (**b**) SINTACS-LU method.

According to the procedure [3], the results of the SINTACS parameters elaboration show that the groundwater vulnerability index ranges from 62 to 185; it was classified into low (<105), moderate (106–140) and high (>140) vulnerability classes [3] (Figure 5a). The results even indicated that the low, moderate and high groundwater vulnerability zones cover 7%, 51% and 42% of the study area, respectively. The application highlights that more than half of the study area is at moderate vulnerability in terms of intrinsic susceptibility to pollution (Figure 6a).

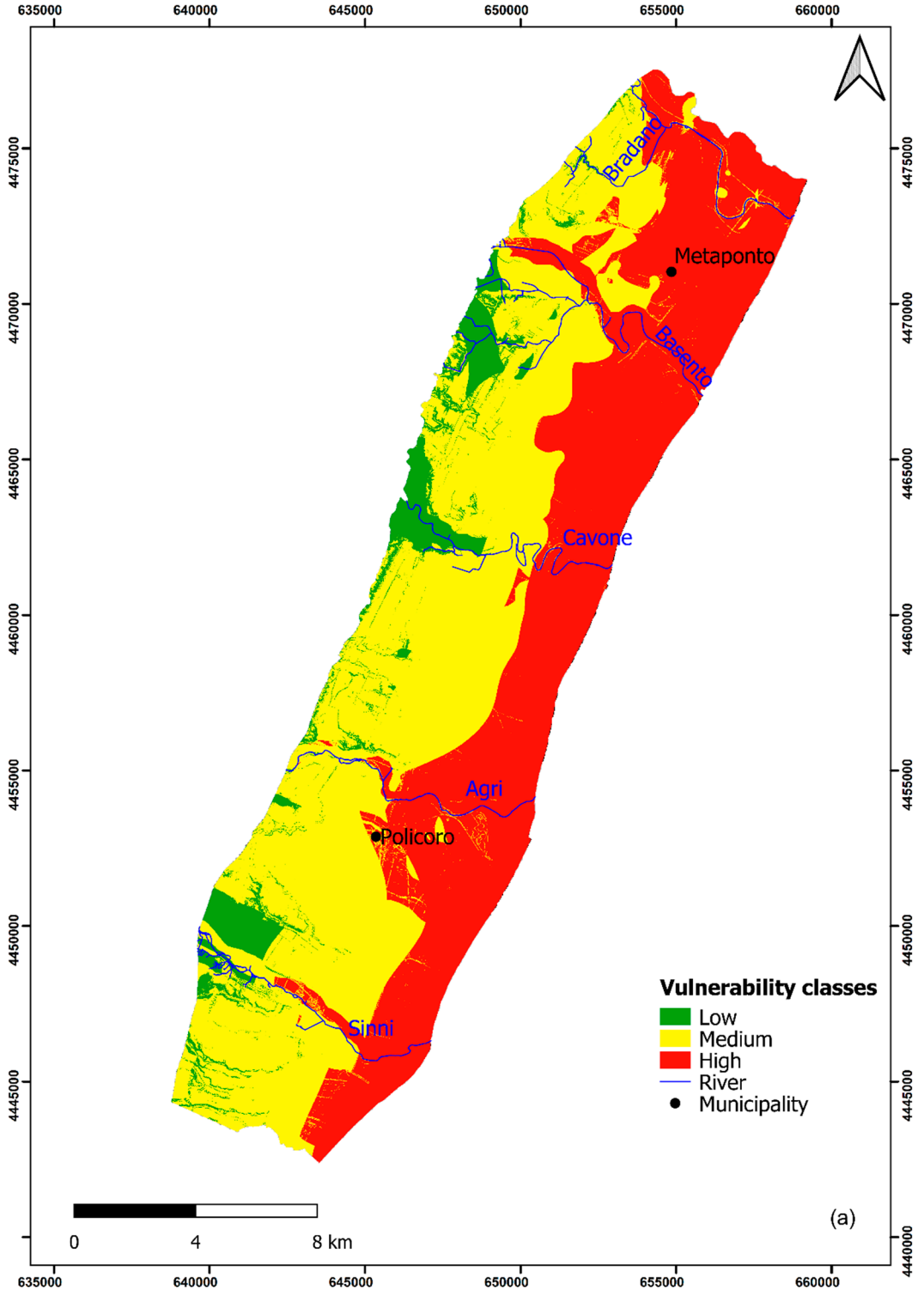

Figure 6. *Cont.*

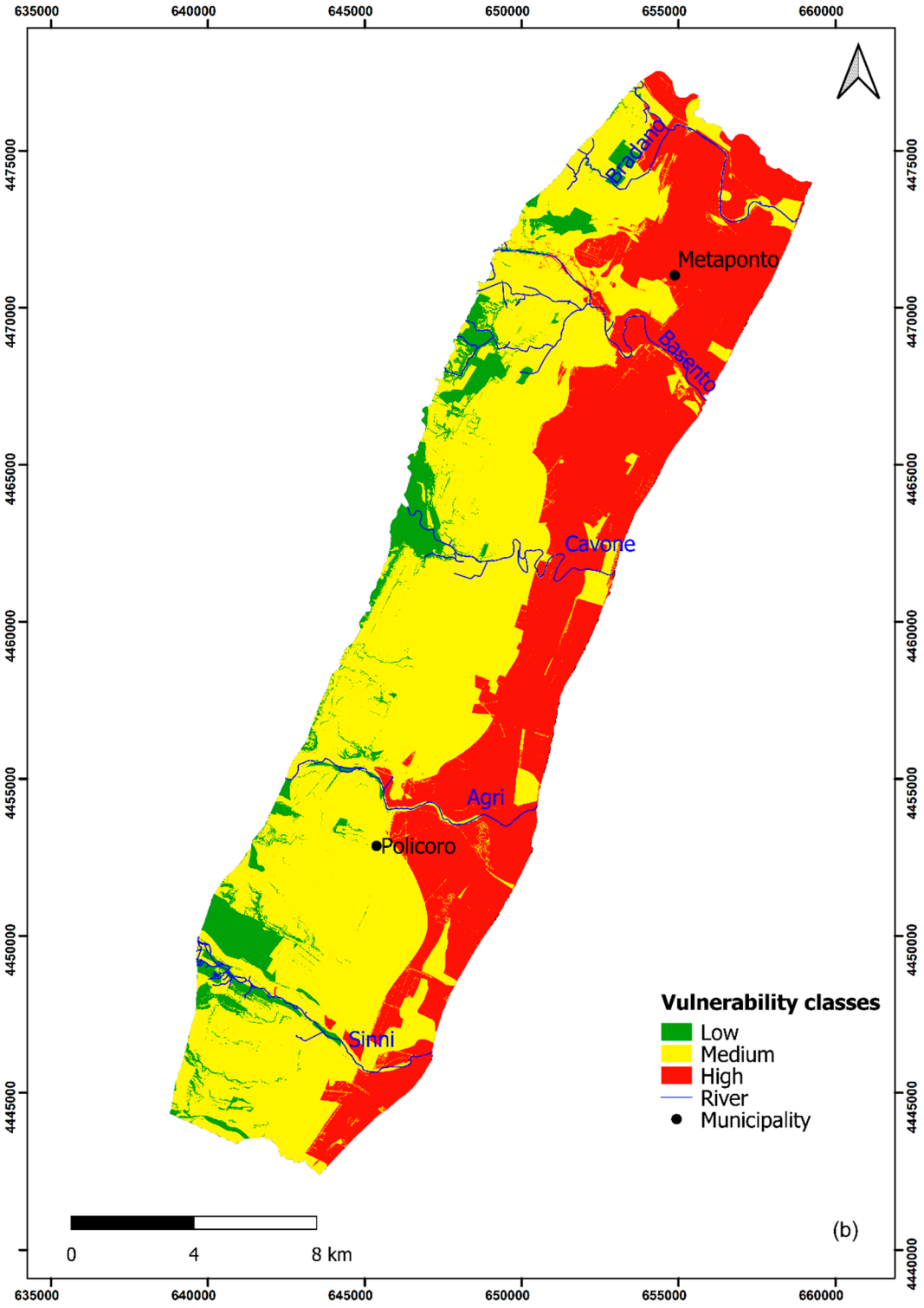

Figure 6. Groundwater vulnerability maps derived from: (**a**) SINTACS and (**b**) SINTACS-LU methods.

By a combination of the eight thematic layers in the GIS-based SINTACS-LU method, the intrinsic vulnerability index was calculated. The elaboration carried out considering the LU parameter shows that the vulnerability index ranges from 77 to 215 (Figure 5b).

Since the SINTACS and SINTACS-LU indexes do not vary in the same range, they have been normalized to allow the vulnerability zonation. The normalization of the SIN-

TACS and SINTACS-LU indexes of the single cells was performed based on the following equation [3,26,44]:

$$I_{norm} = \left[\frac{I - I_{min}}{I_{max} - I_{norm}}\right] \cdot 100, \quad (5)$$

where I_{norm} is the normalized index, and I_{min} and I_{max} are the minimum and maximum values of the indexes, respectively.

The groundwater vulnerability map resulting in the application and normalization of the SINTACS-LU classifies the majority of the plain (56%) as moderate vulnerability. Seven percent of the study area is classified as low and the 37% of the study area as high vulnerability (Figure 6b).

SINTACS and SINTACS-LU results classified as a very high vulnerability class in any part of the study area.

Low vulnerability areas, situated at a small scale in the upper part of the hydrogeological basin, showed low ratings of the water depth and soil media, despite high ratings of the hydraulic conductivity and effective infiltration. Part of the northwestern and the central sides show diffuse moderate vulnerability. The southeastern side shows high vulnerability due to the effects of the shallow water table, the small thicknesses of the unsaturated zones and the soil media typologies.

The vulnerability classes of both methods pointed out comparable pattern. In the SINTACS-LU approach, a great land use impact was noticed due to the high weight assigned to it.

The use of fertilizers in agricultural activities can be recognized as a source of nitrate contamination in the study area. Hence, the consideration of the land use as a vulnerability conditioning parameter and the "Nitrates" string of weight are significantly representative of the actual land use condition and implies the effective suitability of SINTACS-LU for assessing groundwater vulnerability in the study area. The comparison between SINTACS and SINTACS-LU results, highlights that the SINTACS-LU method takes into account the specific characteristics of the land use that plays an essential role in groundwater vulnerability evaluation.

The southeastern part is classified as highly vulnerable on both maps. The lowest vulnerable portions, located in the north-western and southern zones of the study area, are similarly distributed in both maps. The intensive agricultural, industrial and other anthropogenic activities with the peculiar hydrogeological characteristics of the aquifer system favor the high vulnerability to contamination. In the SINTACS-LU map some areas, classified as highly vulnerable in the SINTACS method, show a minor vulnerability class. These areas are situated in natural and forest sectors of the Metaponto plain, which are less populated, and where human impact on the groundwater is limited.

5.3. Sensitivity Analysis

5.3.1. Map Removal

In the map removal sensitivity analysis, each SINTACS and SINTACS-LU parameter was removed one at a time to see how it affected the output. The effect is expressed in terms of the variation index [72] calculated in each cell of the study area by Equation (3). Tables 3 and 4 give a statistical overview of the variation index resulting from the removal of each parameter. The mean of the variation index in all cells for each variable was used to evaluate the sensitivity of that variable if omitted.

Table 3. Statistical summary of the SINTACS map removal sensitivity analysis.

Variation Index (%)	Variable Removed						
	S	**I**	**N**	**T**	**A**	**C**	**S**
Mean	1.44	2.99	1.37	1.22	2.23	1.90	0.78
Minimum	0.00	0.74	0.00	0.00	0.00	0.00	0.00
Maximum	4.56	8.01	7.38	5.92	7.80	5.30	7.76
SD	0.82	1.02	1.28	1.13	1.08	0.96	0.82

Table 4. Statistical summary of the SINTACS-LU map removal sensitivity analysis.

Variation Index (%)	Variable Removed							
	S	**I**	**N**	**T**	**A**	**C**	**S**	**LU**
Mean	1.08	1.26	0.27	0.46	0.78	0.58	0.46	2.03
Minimum	0.30	0.14	0.00	0.00	0.12	0.00	0.00	0.01
Maximum	2.98	1.48	1.08	2.47	1.31	1.16	1.55	5.41
SD	0.52	0.22	0.17	0.38	0.14	0.27	0.22	1.01

For the SINTACS method, the removal of the effective infiltration (I) parameter caused the largest variation index, with a mean of 2.99%. Aquifer media (A) and hydraulic conductivity (C), with mean values of 2.23% and 1.90%, respectively, were the other parameters with higher variation indexes. In descending order, the other parameters are the depth of the water table (S), unsaturated zone (N) and soil media (T). With a variation index of 0.78%, Topography (S) had the lowest means.

In the SINTACS-LU approach, the removal of the land use (LU) parameter caused the highest variation index, with a mean of 2.03%. In descending order, the other parameters are the effective infiltration (I), depth of the water table (S), aquifer media (A), hydraulic conductivity (C), soil media (T), and topography (S). The unsaturated zone (N), with a variation index of 0.27%, had the lowest mean.

5.3.2. Single-Parameter Sensitivity Analysis

Tables 5 and 6 show for each variable the statistics of the single-parameter sensitivity analysis: the theoretical weight originally assigned by SINTACS and SINTACS-LU methods, the same weight normalized to 100, the average effective weight computed on the entire study area, the standard deviation and the minimum and maximum values.

Table 5. Statistical summary of the SINTACS single-parameter sensitivity analysis.

Parameter	Theoretical Weight	Theoretical Weight (%)	Average Effective Weight (%)	Standard Deviation (%)	Minimum Value (%)	Maximum Value (%)
S	5	19.23	27.17	3.33	19.87	48.39
I	5	19.23	5.17	2.55	2.63	15.63
N	4	15.38	14.99	1.74	8.42	24.10
T	5	19.23	19.36	4.12	9.26	39.13
A	2	7.69	9.70	1.84	5.36	16.28
C	2	7.69	11.69	3.39	5.62	29.03
S	3	11.54	20.71	4.30	2.10	37.50

In both methods, almost all parameters showed an effective weight higher than the theoretical one. The effective infiltration (I) showed effective weight was significantly lower than theoretical one, whereas the unsaturated zone (N) and soil media (T) showed the lowest differences between the effective and theoretical weights.

For SINTACS method, the depth of the water table (S) mostly influenced the final vulnerability index, with an average weight of 27.17%, in agreement with the highest theoretical weight of 19.23%. On the contrary, the effective infiltration (I), which together

with the depth of the water table (S) and soil media (T) had the highest theoretical weight, had the lowest effective weight with an average value of 5.17%.

Table 6. Statistical summary of the SINTACS-LU single-parameter sensitivity analysis.

Parameter	Theoretical Weight	Theoretical Weight (%)	Average Effective Weight (%)	Standard Deviation (%)	Minimum Value (%)	Maximum Value (%)
S	5	16.13	23.35	3.19	16.85	50.85
I	5	16.13	4.41	2.10	2.30	16.13
N	4	12.90	12.89	1.67	6.90	25.00
T	5	16.13	16.69	3.99	7.94	40.18
A	2	6.45	8.31	1.50	4.48	16.87
C	2	6.45	10.00	2.83	4.61	30.51
S	3	9.68	17.74	3.48	1.76	32.88
LU	5	16.13	23.95	6.40	8.02	47.62

In the SINTACS-LU approach, the land use (LU) was the most effective parameter on the final vulnerability index (average weight 23.95%), coherently with the highest theoretical weight of 16.13%, in agreement with the results of the map removal sensitivity analysis. On the other hand, as for the SINTACS method, the effective infiltration (I), which together with the depth of the water table (S), soil media (T), and land use (LU) had the highest theoretical weight and had the lowest effective weight with an average value of 4.41%.

6. Conclusions

In the present paper, the overlay and index methods SINTACS and SINTACS-LU were applied for assessing the groundwater vulnerability of the Metaponto coastal plain. The land use parameter was added because of its importance in the study area and its impact on groundwater vulnerability. The groundwater vulnerability to pollution of the study area was classified into low, moderate and high classes.

The sector classified as highly vulnerable is closest to the sea and represents the area that most needs opportune management of groundwater resources.

Map removal and single-parameter were the two types of sensitivity analysis performed in this research to understand the influence of the input parameters on the output.

The assessment of the intrinsic vulnerability of the Metaponto coastal plain aquifer will assist in prioritizing groundwater protection measures and help in the selection of the most vulnerable areas for further investigation and monitoring. This is more important, considering that vulnerability assessment is gaining increasing attention because of the key role that groundwater quality plays in the study area.

The knowledge of potential intrinsic vulnerability and the issues related to the quality of groundwater represents a significant task to prevent and control the pollution of the resources. Indeed, the identification of the aquifer zones characterized by high vulnerability represents an important step useful for both groundwater management and communities' awareness concerning the resulting environmental problems.

Furthermore, this study leads to new considerations concerning the link of the aquifer hydrogeological behavior to the anthropogenic activities, related to the release of the pollutants in the subsurface, and climate change. For understanding these issues, future studies should consider the factors influencing the hydrogeological situations in responding to changing conditions, with particular attention to the effects of climate change on groundwater resources that could determine negative impacts in terms of both quantity and quality.

Author Contributions: Investigation, data analysis, methodology application and writing—original draft F.C. and R.M.; writing—review F.C., R.M. and F.S.; supervision F.C. and F.S. All authors have read and agreed to the published version of the manuscript.

Funding: This research received no external funding.

Institutional Review Board Statement: Not applicable.

Informed Consent Statement: Not applicable.

Data Availability Statement: The data presented in this study are available on request from the corresponding author.

Acknowledgments: The authors are grateful to the reviewers of this paper for their constructive comments and valuable suggestions, which greatly improved the quality of the manuscript.

Conflicts of Interest: The authors declare no conflict of interest.

References

1. WHO (World Health Organization). *Guidelines for Drinking-Water Quality: Fourth Edition Incorporating First Addendum*; WHO: Geneva, Switzerland, 2017; p. 631.
2. Adams, B.; Foster, S.S.D. Land-surface zoning for groundwater protection. *J. Inst. Water Environ. Manag.* **1992**, *6*, 312–320. [CrossRef]
3. Civita, M.; De Maio, M. *SINTACS. Un Sistema Parametrico per la Valutazione e la Cartografia Della Vulnerabilità Degli Acquiferi All'inquinamento. Metodologia e Automazione, Quaderni di Tecniche di Protezione Ambientale*; Pitagora Editrice: Bologna, Italy, 1997; p. 191.
4. Kumar, A.; Krishna, A.P. Groundwater vulnerability and contamination risk assessment using GIS-based modified DRASTIC-LU model in hard rock aquifer system in India. *Geocarto Int.* **2018**, *35*, 1149–1178. [CrossRef]
5. Barbulescu, A. Assessing Groundwater Vulnerability: DRASTIC and DRASTIC-Like Methods: A Review. *Water* **2020**, *12*, 1356. [CrossRef]
6. Kirlas, M.C.; Karpouzos, D.K.; Georgiou, P.E.; Katsifarakis, K.L. A comparative study of groundwater vulnerability methods in a porous aquifer in Greece. *Appl. Water Sci.* **2022**, *12*, 123. [CrossRef]
7. Mendoza, J.A.; Barmen, G. Assessment of groundwater vulnerability in the Río Artiguas basin, Nicaragua. *Environ. Geol.* **2006**, *50*, 569–580. [CrossRef]
8. Albinet, M.; Margat, J. Cartographie de la vulnerabilité de à la pollution des nappes d'eau souterraine. *Orléans France. Bull. BRGM* **1970**, *4*, 13–22.
9. Vrba, J.; Zaporozec, A. Guidebook on Mapping Groundwater Vulnerability. In *IAH International Contributions to Hydrogeology*; Heise Pub.: Hannover, Germany, 1994; Volume 16, p. 131.
10. National Research Council. *Ground Water Vulnerability Assessment: Predicting Relative Contamination Potential under Conditions of Uncertainty*; The National Academy Press: Washington, DC, USA, 1993. [CrossRef]
11. Civita, M. La previsione e la prevenzione del rischio di inquinamento delle acque sotterranee a livello regionale mediante le Carte di Vulnerabilità. In Proceedings of the Conference Inquinamento delle Acque Sotterranee: Previsione e Prevenzione, Mantova, Italy, 11 February 1987; pp. 9–18.
12. Zwahlen, F. *Vulnerability and Risk Mapping for the Protection of Carbonate (Karst) Aquifers, Final Report (COST Action 620)*; Report EUR 20912; European Commission: Brussels, Belgium, 2004; p. 297.
13. Machiwal, D.; Cloutier, V.; Güler, C.; Kazakis, N. A review of GIS-integrated statistical techniques for groundwater quality evaluation and protection. *Environ. Earth Sci.* **2018**, *77*, 681. [CrossRef]
14. Machiwal, D.; Jha, M.K.; Singh, V.P.; Mohan, C. Assessment and mapping of groundwater vulnerability to pollution: Current status and challenges. *Earth-Sci. Rev.* **2018**, *185*, 901–927. [CrossRef]
15. Taghavi, N.; Niven, R.K.; Paull, D.J.; Kramer, M. Groundwater vulnerability assessment: A review including new statistical and hybrid methods. *Sci. Total Environ.* **2022**, *822*, 153486. [CrossRef]
16. Jha, M.K.; Chowdhury, A.; Chowdary, V.M.; Peiffer, S. Groundwater management and development by integrated remote sensing and geographic information systems: Prospects and constraints. *Water Resour. Manag.* **2007**, *21*, 427–467. [CrossRef]
17. Voss, C.I. *A Finite Element Simulation Model for Saturated-Unsaturated Fluid Density-Dependent Groundwater Flow with Energy Transport or Chemically Reactive Single-Species Solute Transport*; U.S. Geological Survey: Reston, VA, USA, 1984.
18. Carsel, R.F.; Mulkey, L.A.; Lorber, M.N.; Baskin, L.B. The pesticide root zone model (PRZM): A procedure for evaluating pesticide leaching threats to ground water. *Ecol. Model.* **1985**, *30*, 49–69. [CrossRef]
19. Wagenet, R.J.; Hutson, J.L. Predicting the fate of non-volatile pesticides in the unsaturated zone. *J. Environ. Qual.* **1986**, *15*, 315–322. [CrossRef]
20. Leonard, R.A.; Knisel, W.G.; Still, D.A. GLEAMS: Groundwater loading effects of agricultural management systems. *Trans. Am. Soc. Agric. Eng.* **1987**, *30*, 1403–1418. [CrossRef]
21. Zheng, C.; Wang, P.P. *MT3DMS: A Modular Three-Dimensional Multispecies Transport Model for Simulation of Advection, Dispersion, and Chemical Reactions of Contaminants in Groundwater Systems*; Documentation and User's Guide; Contract Report SERDP-99-1; U.S. Army Engineer Research and Development Center: Vicksburg, MS, USA, 1999.
22. Šimunek, J.; Šejna, M.; van Genuchten, M.T. *The HYDRUS-1D Software Package for Simulating the One-Dimensional Movement of Water, Heat, and Multiple Solutes in Variably-Saturated Media*; University of California: Riverside, CA, USA, 2005; p. 240.

23. Aller, L.; Bennett, T.; Lehr, J.H.; Petty, R.J.; Hackett, G. *DRASTIC: A Standardized System for Evaluating Ground Water Pollution Potential Using Hydrogeologic Settings*; U.S. Environmental Protection Agency: Washington, DC, USA, 1987; p. 455.
24. Civita, M. *Idrogeologia Applicata e Ambientale*; CEA: Milano, Italy, 2005; pp. 1–794.
25. Civita, M.; De Maio, M. *SINTACS R5 a New Parametric System for the Assessment and Automatic Mapping of Groundwater Vulnerability to Contamination*; Pitagora Editrice: Bologna, Italy, 2000; p. 226.
26. Civita, M.; De Maio, M. Assessing and mapping groundwater vulnerability to contamination: The Italian "combined" approach. *Geofísica Int.* **2004**, *43*, 513–532. [CrossRef]
27. Doerfliger, N.; Jeannin, P.Y.; Zwahlen, F. Water vulnerability assessment in karst environments: A new method of defining protection areas using a multi-attribute approach and GIS tools (EPIK method). *Environ. Geol.* **1999**, *39*, 165–176. [CrossRef]
28. Vías, J.; Andreo, B.; Perles, M.; Carrasco, F.; Vadillo, I.; Jiménez, P. Proposed method for groundwater vulnerability mapping in carbonate (karstic) aquifers: The COP method. *Hydrogeol. J.* **2006**, *14*, 912–925. [CrossRef]
29. Nolan, B.T.; Hitt, K.J.; Ruddy, B.C. Probability of nitrate contamination of recently recharged groundwaters in the conterminous United States. *Environ. Sci. Technol.* **2002**, *36*, 2138–2145. [CrossRef]
30. Twarakavi, N.K.C.; Kaluarachchi, J.J. Aquifer vulnerability assessment to heavy metals using ordinal logistic regression. *Ground Water* **2005**, *43*, 200–214. [CrossRef]
31. Rupert, M.G. Calibration of the DRASTIC ground water vulnerability mapping method. *Ground Water* **2001**, *39*, 625–630. [CrossRef]
32. Gupta, P.K.; Kumari, B.; Gupta, S.K.; Kumar, D. Nitrate-leaching and groundwater vulnerability mapping in North Bihar, India. *Sustain. Water Resour. Manag.* **2020**, *6*, 48. [CrossRef]
33. Javadinejad, S.; Ostad-Ali-Askari, K.; Jafary, F. Using simulation model to determine the regulation and to optimize the quantity of chlorine injection in water distribution networks. *Model. Earth Syst. Environ.* **2019**, *5*, 1015–1023. [CrossRef]
34. Ostad-Ali-Askari, K.; Shayannejad, M.; Ghorbanizadeh-Kharazi, H. Artificial neural network for modeling nitrate pollution of groundwater in marginal area of Zayandeh-rood River, Isfahan, Iran. *KSCE J. Civ. Eng.* **2017**, *21*, 134–140. [CrossRef]
35. Ostad-Ali-Askari, K.; Shayannejad, M. Quantity and quality modelling of groundwater to manage water resources in Isfahan-Borkhar Aquifer. *Environ. Dev. Sustain.* **2021**, *23*, 15943–15959. [CrossRef]
36. Tesoriero, A.J.; Voss, F.D. Predicting the probability of elevated nitrate concentrations in the Puget Sound Basin: Implications for aquifer susceptibility and vulnerability. *Groundwater* **1997**, *35*, 1029–1039. [CrossRef]
37. Stevenazzi, S.; Bonfanti, M.; Masetti, M.; Nghiem, S.V.; Sorichetta, A. A versatile method for groundwater vulnerability projections in future scenarios. *J. Environ. Manag.* **2017**, *187*, 365–374. [CrossRef]
38. Sahoo, S.; Dhar, A.; Kar, A.; Chakraborty, D. Index-based groundwater vulnerability mapping using quantitative parameters. *Environ. Earth Sci.* **2016**, *75*, 522. [CrossRef]
39. Kazakis, N.; Voudouris, K.S. Groundwater vulnerability and pollution risk assessment of porous aquifers to nitrate: Modifying the DRASTIC method using quantitative parameters. *J. Hydrol.* **2015**, *525*, 13–25. [CrossRef]
40. Panagopoulos, G.; Antonakos, A.; Lambrakis, N. Optimization of the DRASTIC method for groundwater vulnerability assessment via the use of simple statistical methods and GIS. *Hydrogeol. J.* **2006**, *14*, 894–911. [CrossRef]
41. Brindha, K.; Elango, L. Cross comparison of five popular groundwater pollution vulnerability index approaches. *J. Hydrol.* **2015**, *524*, 597–613. [CrossRef]
42. Jahromi, M.N.; Gomeh, Z.; Busico, G.; Barzegar, R.; Samany, N.N.; Aalami, M.T.; Tedesco, D.; Mastrocicco, M.; Kazakis, N. Developing a SINTACS-based method to map groundwater multi-pollutant vulnerability using evolutionary algorithms. *Environ. Sci. Pollut. Res.* **2021**, *28*, 7854–7869. [CrossRef]
43. Civita, M. *Le Carte della Vulnerabilità Degli Acquiferi All'inquinamento: Teoria e Pratica, Quaderni di Tecniche di Protezione Ambientale*; Pitagora Editrice: Bologna, Italy, 1994; pp. 325–333.
44. Civita, M. The combined approach when assessing and mapping groundwater vulnerability to contamination. *J. Water Resour. Prot.* **2010**, *2*, 14–28. [CrossRef]
45. Noori, R.; Ghahremanzadeh, H.; Kløve, B.; Adamowski, F.J.; Baghvand, A. Modified-DRASTIC, modified-SINTACS and SI methods for groundwater vulnerability assessment in the southern Tehran aquifer. *J. Environ. Sci. Health* **2019**, *54*, 89–91. [CrossRef] [PubMed]
46. Eftekhari, M.; Akbari, M. Evaluation of the SINTACS-LU model capability in the analysis of aquifer vulnerability potential in semiarid regions. *J. Appl. Res. Water Wastewater* **2020**, *7*, 111–119.
47. Jesudhas, C.J.; Chinnasamy, A.; Muniraj, K.; Sundaram, A. Assessment of vulnerability in the aquifers of rapidly growing sub-urban: A case study with special reference to land use. *Arab. J. Geosci.* **2021**, *14*, 60. [CrossRef]
48. Longhitano, S.G. Short-Term Assessment of Retreating vs. Advancing Microtidal Beaches Based on the Backshore/Foreshore Length Ratio: Examples from the Basilicata Coasts (Southern Italy). *Open J. Mar. Sci.* **2015**, *5*, 123–145. [CrossRef]
49. Cilumbriello, A.; Sabato, L.; Tropeano, M.; Gallicchio, S.; Grippa, A.; Maiorano, P.; Mateu-Vicens, G.; Rossi, C.A.; Spilotro, G.; Calcagnile, L.; et al. Sedimentology, stratigraphic architecture and preliminary hydrostratigraphy of the Metaponto coastal-plain subsurface (Southern Italy). In *Proceedings of the National Workshop Multidisciplinary Approach for Porous Aquifer Characterization*; Bersezio, R., Amanti, M., Eds.; Memorie Descrittive della Carta Geologica d'Italia: Rome, Italy, 2010; pp. 67–84.
50. Gioia, D.; Bavusi, M.; Di Leo, P.; Giammatteo, T.; Schiattarella, M. Geoarchaeology and geomorphology of the Metaponto area, Ionian coastal belt, Italy. *J. Maps* **2020**, *16*, 117–125. [CrossRef]

51. Pescatore, T.; Pieri, P.; Sabato, L.; Senatore, M.R.; Gallicchio, S.; Boscaino, M.; Cilumbriello, A.; Quarantiello, R.; Capretto, G. Stratigrafia dei depositi pleistocenico-olocenici dell'area costiera di Metaponto compresa fra Marina di Ginosa ed il Torrente Cavone (Italia meridionale): Carta geologica in scala 1:25,000. *Il Quat.* **2009**, *22*, 307–324.
52. Tropeano, M.; Sabato, L.; Pieri, P. The Quaternary «Post-turbidite» sedimentation in the South-Apennines Foredeep (Bradanic Trough-Southern Italy). *Boll. Soc. Geol. Ital.* **2002**, *1*, 449–454.
53. Tropeano, M.; Cilumbriello, A.; Sabato, L.; Gallicchio, S.; Grippa, A.; Longhitano, S.G.; Bianca, M.; Gallipoli, M.R.; Mucciarelli, M.; Spilotro, G. Surface and subsurface of the Metaponto coastal plain (Gulf of Taranto—Southern Italy): Present-day- vs. *LGM landscape. Geomorphol.* **2013**, *203*, 115–131. [CrossRef]
54. Geological Survey of Italy. *Geological Map of Italy, 1:100,000 Scale*; ISPRA—Land Protection and Georesources Department: Rome, Italy, 1976.
55. Geological Survey of Italy. *Geological Map of Italy, 1:50,000 Scale*; ISPRA—Land Protection and Georesources Department: Rome, Italy, 2016.
56. Parea, G.C. I terrazzi marini tardo-pleistocenici del fronte della catena appenninica in relazione alla geologia dell'avanfossa adriatica (The Late Pleistocene marine terraces in front of the Apennines in relation to the geology of Adriatic Foredeep). *Mem. Soc. Geol. Ital.* **1986**, *35*, 913–936.
57. Cocco, E.; Cravero, E.; Di Geronimo, S.; Mezzadri, G.; Parea, G.C.; Pescatore, T.; Valloni, R.; Vinci, A. Lineamenti geomorfologici e sedimentologici del litorale alto ionico (Golfo di Taranto). *Boll. Soc. Geol. Ital.* **1975**, *94*, 993–1051.
58. Radina, B. Idrogeologia del Bacino del fiume Basento. *Mem. Sc. Geol.* **1969**, *21*, 52.
59. Polemio, M.; Limoni, P.P.; Mitolo, D.; Santaloia, F. Characterisation of the ionian-lucanian coastal plain aquifer (Italy). *Bol. Geol. Y Min.* **2003**, *114*, 225–236.
60. Muzzillo, R.; Zuffianò, L.E.; Rizzo, E.; Canora, F.; Capozzoli, L.; Giampaolo, V.; De Giorgio, G.; Sdao, F.; Polemio, M. Seawater Intrusion Proneness and Geophysical Investigations in the Metaponto Coastal Plain (Basilicata, Italy). *Water* **2021**, *13*, 53. [CrossRef]
61. Polemio, M.; Limoni, P.P.; Mitolo, D.; Santaloia, F.; Virga, R. Nitrate pollution and quality degradation of Ionian coastal groundwater (Southern Italy). In *Nitrates in Groundwater*; Razowska-Jaworek, L., Sadurski, A., Eds.; CRC Press: Rotterdam, The Netherlands, 2005; pp. 163–176.
62. Hamza, M.H.; Added, A.; Francés, A.; Rodríguez, R. Validité de l'application des méthodes de vulnérabilité drastic, sintacs et SI à l'étude de la pollution par les nitrates dans la nappe phréatique de Metline–Ras Jebel–Raf Raf (Nord-Est tunisien). *Comptes. Rendus Geosci.* **2007**, *339*, 493–505. [CrossRef]
63. Webster, R.; Oliver, M.A. *Geostatistics for Environmental Scientists*; John Wiley & Sons: Chichester, UK, 2007; p. 330.
64. De Marsily, G. Spatial Variability of Properties in Porous Media: A Stochastic Approach. In *Fundamentals of Transport in Porous Media*; Bear, J., Corapcioglu, M.Y., Eds.; Martinus Nijhoff: Leiden, The Netherlands, 1984; pp. 719–769.
65. Canora, F.; Musto, M.A.; Sdao, F. Groundwater recharge assessment in the carbonate aquifer system of the Lauria Mounts (southern Italy) by GIS-based distributed hydrogeological balance method. In *Computational Science and Its Applications*; ICCSA 2018, Lecture Notes in Computer Science; Springer: Cham, Switzerland, 2018; Volume 10961, pp. 166–181. [CrossRef]
66. Canora, F.; Sdao, F. Hydrogeological characterization and groundwater vulnerability to pollution assessment of the High Basento River Valley carbonate hydrostructure (Southern Italy). *Ital. J. Eng. Geol. Environ.* **2020**, *1*, 25–44.
67. Muzzillo, R.; Zuffiano, L.E.; Canora, F.; De Giorgio, G.; Limoni, P.P.; Polemio, M.; Sdao, F. Hydrogeology and seawater intrusion proneness in the Metaponto plain aquifer (Basilicata, Italy). *Ital. J. Eng. Geol. Environ.* **2021**, *1*, 139–149. [CrossRef]
68. Regione Basilicata. *I Suoli Della Basilicata*; S.E.L.C.A.: Firenze, Italy, 2006; p. 340.
69. CORINE Land Cover (C.L.C.). *European Union, Copernicus Land Monitoring Service 2018*; European Environment Agency (EEA): Copenhagen, Denmark, 2018.
70. Napolitano, P.; Fabbri, A.G. Single-parameter sensitivity analysis for aquifer vulnerability assessment using DRASTIC and SINTACS. In *HydroGIS 96: Application of Geographical Information Systems in Hydrology and Water Resources Management, Proceedings of the Vienna Conference, Vienna, Austria, 16–19 April 1996*; IAHS Pub.: Wallingford, UK, 1996; Volume 235, pp. 559–566.
71. Lodwick, W.A.; Monson, W.; Svoboda, L. Attribute error and sensitivity analysis of map operations in geographical information systems: Suitability analysis. *Int. J. Geogr. Inf. Syst.* **1990**, *4*, 413–428. [CrossRef]
72. Babiker, I.S.; Mohamed, M.A.A.; Hiyama, T.; Kato, K. A GIS-based DRASTIC model for assessing aquifer vulnerability in Kakamigahara Heights, Gifu Prefecture, central Japan. *Sci. Total Environ.* **2005**, *345*, 127–140. [CrossRef]
73. Majandang, J.; Sarapirome, S. Groundwater vulnerability assessment and sensitivity analysis in Nong Rua, Khon Kaen, Thailand, using a GIS-based SINTACS model. *Environ. Earth Sci.* **2013**, *68*, 2025–2039. [CrossRef]
74. Celico, P. *Prospezioni Idrogeologiche*; Liguori: Napoli, Italy, 1988; pp. 1–536.
75. Ckakraborty, S.; Paul, P.K.; Sikdar, P.K. Assessing aquifer vulnerability to arsenic pollution using DRASTIC and GIS of North Bengal Plain: A case study of English Bazar Block, Malda District, West Bengal, India. *J. Spat. Hydrol.* **2007**, *7*, 101–121.
76. Canora, F.; D'Angella, A.; Aiello, A. Quantitative assessment of the sensitivity to desertification in the Bradano River basin (Basilicata, southern Italy). *J. Maps* **2015**, *11*, 745–759. [CrossRef]